Excitonic Zeeman effect in the zinc-blende II-VI diluted magnetic semiconductors $Cd_{1-x}Y_xTe$ (Y=Mn, Co, and Fe)

H. Alawadhi, I. Miotkowski, V. Souw, M. McElfresh, and A. K. Ramdas
Department of Physics, Purdue University, West Lafayette, Indiana 47907

S. Miotkowska
Institute of Physics, Polish Academy of Sciences, Aleja Lotnikow 32/46, 02-668 Warsaw, Poland
(Received 20 April 2000; revised manuscript received 14 July 2000; published 26 March 2001)

The sp-d exchange constants ($N_0\alpha$ and $N_0\beta$) of the zinc-blende diluted magnetic semiconductors $Cd_{1-x}Mn_xTe$, $Cd_{1-x}Co_xTe$, and $Cd_{1-x}Fe_xTe$ are deduced from the huge excitonic Zeeman effect observed in wavelength-modulated reflectivity spectra, supplemented with magnetization measurements with a superconducting quantum interference device magnetometer. The Zeeman spectra recorded in magnetic fields (H) up to 60 kG, and temperatures (T) down to 1.8 K clearly reveal the Van Vleck paramagnetism of $Cd_{1-x}Fe_xTe$; in contrast, $Cd_{1-x}Mn_xTe$ and $Cd_{1-x}Co_xTe$ display a Brillouin-function-like (H/T) dependence of their excitonic Zeeman components associated with spin 5/2 and 3/2 ground states of Mn^{2+} and Co^{2+}, respectively. The antiferromagnetic d-d interaction between the magnetic ions, displayed in the Zeeman data, is mainly limited to nearest-neighbor Mn^{2+} ions, whereas it is significantly stronger for Co^{2+} than for Mn^{2+} and extends to more distant neighbors.

DOI: 10.1103/PhysRevB.63.155201 PACS number(s): 71.70.Ej, 75.50.Pp, 78.20.Ls

I. INTRODUCTION

Tetrahedrally coordinated II-VI multinary alloys in which a fraction of the group-II cations is randomly replaced with $3d$ transition-metal ions, as in $Cd_{1-x}Mn_xTe$ and $Cd_{1-x-y}Zn_yMn_xTe$, are known as diluted magnetic semiconductors (DMS's).[1] In contrast to the nonmagnetic II-VI alloys, DMS's are singled out by their remarkable magnetic and magneto-optic properties, originating in (1) the exchange interaction between the spins of the $3d$ electrons of the transition-metal ions (TMI's) and those of the band electrons,[2] i.e., in the so-called *sp-d exchange interaction*, and (2) the magnetic interaction between the $3d$ electrons of neighboring TMI's, the *d-d exchange interaction*, known to occur through an antiferromagnetic (AF) interaction.

The excitonic Zeeman effect in DMS's is a spectroscopic phenomenon ideally suited for probing the magnetization resulting from the sp-d and d-d interactions. It is also microscopic phenomenon that underlies the giant Faraday and large Voigt effect they display.[3–5] These considerations provide a strong motivation for the study of the excitonic Zeeman effect in II-VI DMS's involving the $3d$ magnetic ions. The excitonic Zeeman effect has been investigated with photoluminescence,[6] in absorption,[7] and in unmodulated reflectivity. The limitations of these techniques (a partial picture of the Zeeman effect, the need for extremely thin samples, or the presence of a large continuum background) are elegantly circumvented by employing one of the many modulation techniques.[8–10] The rather limited studies on TMI's other than Mn^{2+} are due to their low solubility in DMS's based on them. However, the high sensitivity of modulation techniques offers an opportunity for the investigation of the excitonic Zeeman effect in such DMS's even for small x, for example, in $Cd_{1-x}Co_xTe$ and $Cd_{1-x}Fe_xTe$. An intercomparison of Mn^{2+}, Co^{2+}, and Fe^{2+}, each with their characteristic ground-state multiplets as reflected in the excitonic Zeeman effect of $Cd_{1-x}Mn_xTe$, $Cd_{1-x}Co_xTe$, and $Cd_{1-x}Fe_xTe$, is particularly attractive.

In the context of the above considerations, we have carried out a comprehensive study of the excitonic Zeeman effect in the CdTe-based zinc-blende DMS's involving Mn^{2+}, Co^{2+}, and Fe^{2+} magnetic ions, exploiting the power and sensitivity of modulation techniques; the results, along with their interpretations, are reported in the present paper.

II. EXPERIMENT

All the specimens studied in the present investigation were cleaved from bulk single crystals grown by the vertical Bridgman technique. The ternary alloys were prepared using purified CdTe and required amounts of Mn, Co, or Fe and Te added in stoichiometric proportions. Mn metal was purified by multiple sublimation under dynamic vacuum, but Fe and Co of 99.998% purity were used without further purification. The stoichiometric charge was placed inside a graphite-coated ampoule and sealed off under a dynamic vacuum of 10^{-6} Torr. The ampoules, heated to 1150 °C for about 12 h before the growth commenced, were kept static and the furnace moved vertically at a rate of 1–3 mm/h. The temperature gradient in the growth zone ranged between 3 and 8 °C/cm. In the postgrowth period, the ampoules cooled at the rate of 50 °C/h down to 800 °C, followed by 100 °C/h for the cooling rate down to room temperature.

The excitonic signatures were obtained in reflectivity employing wavelength modulation. Measurements were performed with a SPEX 1870 monochromator, a quartz halogen lamp as a light source, and a silicon photodiode as a detector. With calibration lines from Kr, Ar, Xe, and O discharge lamps, the wavelength accuracy of the monochromator in the entire spectral range of interest was ensured. The wavelength modulation was achieved with a vibrating mirror, incorpo-

rated in the monochromator optics, operating at 85 Hz. A Janis superconducting optical magnet cryostat provided a maximum field of 60 kG; its variable-temperature feature allowed samples to reach temperatures down to 1.8 K.

The magnetization data were taken on a Quantum Design MPMS-5 superconducting quantum interference device (SQUID) magnetometer.[11] The computer-controlled system allows data acquisition for temperatures between 1.8 and 400 K and fields up to 55 kG. The magnetometer is capable of measuring magnetic moments as small as 10^{-7} emu, although a signal $\geqslant 10^{-6}$ emu is preferred. Because of the physical limitation of the pick-up coils in the SQUID, the sample sizes did not exceed a few millimeters in width and 1 mm in thickness (with a mass of about 50 mg).

The composition of the samples was determined using a JEOL JSM-6400 scanning electron microscope[12] equipped with a LINK data analysis system for energy-dispersive electron microprobe analysis (EMPA). The quantitative EMPA results were obtained using CdTe, CdMnTe, and pure Co and Fe as standards. The accuracy of the composition using this technique is estimated to be about 0.05 at. %.

III. THEORETICAL BACKGROUND

The half-filled *d* subshell of Mn is the main reason why it has a simple orbital singlet $^6S_{5/2}$ ground state. But as one goes through the other $3d$ metals on either side of Mn in the periodic table, the departure (excess or deficit) from the half-filled *d* subshell leads to more complex ground states.[13] As a result, DMS's based on these ions show magnetic behavior richer and more complex than that of the Mn-based compounds. The ferromagnetic *p-d* interaction in $Zn_{1-x}Cr_xSe$ (Ref. 14) and the Van Vleck paramagnetism in $Cd_{1-x}Fe_xSe$ (Ref. 15) are unique and intriguing examples of these phenomena.

In considering the excitonic levels of a DMS, one must account for the *intrinsic magnetic interactions* of the host (e.g., CdTe). A direct-gap zinc-blende semiconductor is characterized by a zone center Γ_6 ($J_c=\frac{1}{2}$) conduction-band minimum and a Γ_8 ($J_v=\frac{3}{2}$) valence-band maximum. In the presence of an external magnetic field, the orbital motions of band electrons lead to Landau quantization of the bands and the spin dynamics of the electrons result in a further spin splitting of the Landau levels.[16]

The dramatic magneto-optic effects displayed by a DMS can be traced to the exchange interaction between the localized magnetic moments of the TMI's and those of the band electrons. This effect is taken into account by adding an exchange term, the *sp-d* exchange Hamiltonian $\mathcal{H}_{sp\text{-}d}$, to the zero-field Hamiltonian. The extended nature of the electronic wave function spanning a large number of magnetic ions and lattice sites allows the use of the *molecular-field approximation* to replace the magnetic-ion spin operator $\mathbf{S}_i$ with its thermal and spatial average $\langle\langle \mathbf{S} \rangle\rangle$, taken over all the ions. Also, the exchange interaction can be treated in the spirit of the virtual-crystal approximation, along with its translational symmetry.

When used as perturbations to the zero-field Hamiltonian, the diagonalized Hamiltonians corresponding to the *s-p* and

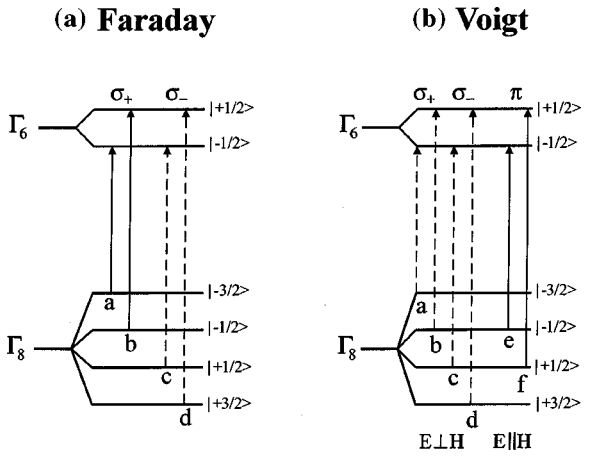

FIG. 1. Exchange splitting of the valence and conduction bands for zinc-blende II-VI DMS's and the excitonic transitions in (a) Faraday ($\mathbf{k}\|\mathbf{H}$) and (b) Voigt geometries ($\mathbf{k}\perp\mathbf{H}$), where $\mathbf{k}$ is the direction of light propagation.

p-d interactions[7] result in a splitting of the conduction band into two subbands and the valence band into four subbands, as shown in Fig. 1. The energies of these subbands, inclusive of the *sp-d* exchange interaction, are given by

$$E_c^{sd}(m_J) = E_c - m_J^c N_0 \alpha x \langle\langle S_z \rangle\rangle,$$

$$E_v^{pd}(m_J) = E_v - \tfrac{1}{3} m_J^v N_0 \beta x \langle\langle S_z \rangle\rangle, \qquad (1)$$

where c and v refer to the conduction and valence bands, respectively, E_c and E_v are the conduction- and valence-band-edge energies in the absence of the exchange interaction, N_0 is the number of unit cells per unit volume, α and β are the *s-d* and *p-d* exchange integrals for the conduction- and valence-band electrons, respectively, and x is the molar fraction of the TMI.

If the mean magnetic moment of the TMI is proportional to its mean spin $\langle S_z \rangle$ in a magnetic field $\mathbf{H}\|\mathbf{z}$, a g factor g_i can be defined for the TMI in the DMS host. The magnetization (per unit mass) due to these magnetic ions is then given by

$$M_m = M_m^* + \chi_{\rm dia} H = -\frac{g_i \mu_B N_A}{W(x)} x \langle\langle S_z \rangle\rangle + \chi_{\rm dia} H, \qquad (2)$$

where N_a is Avogadro's number, μ_B is the Bohr magneton, and $W(x)$ is the molar weight of the DMS. Here M_m^* is the contribution of the magnetic ions to the magnetization, while $\chi_{\rm dia}$ arises from the diamagnetic susceptibility of the host. This small diamagnetic contribution, which is linear in field, should be considered for high values of H/T and low x. For CdTe, $\chi_{\rm dia} = -3.45 \times 10^{-7}$ emu/g.[17]

In Eq. (2), the mean spin $\langle\langle S_z \rangle\rangle$ denotes the spatial as well as the thermal average of the spin component along the magnetic field. Assuming the magnetization of a dilute alloy, in which it is experimentally justified to consider contributions of only two types of complex, *singles* (with no other neighboring magnetic ion) and *pairs* (when two ions are neighbors), and for spin interactions up to the *k*th neighbor,

$$\langle\langle S_z\rangle\rangle_k = P_k^s(x)\langle S_z\rangle_k^s + \sum_{j=1}^{k} P_j^p(x)\langle S_z\rangle_j^p, \tag{3}$$

where the index s refers to isolated ions up to the kth neighbor, and p corresponds to pairs that are first $(j=1),\ldots,k$th $(j=k)$ neighbors. $P_j(x)$ is the probability that a magnetic-ion spin belongs to the complex j. For a random distribution of ions over a fcc sublattice, Kreitman and Barnett[18] and Okada[19] give the probabilities for first-, second-, and third-neighbor interactions.

It is important to consider the special case of a spherically symmetric magnetic ion in a II-VI host. Despite its limitation, this model is applicable, to a good approximation, to $Cd_{1-x}Mn_xTe$ because of the small crystal-field splitting of the Mn^{2+} ground state, and to $Cd_{1-x}Co_xTe$ because of the large crystal-field-induced separation of the first excited state of Co^{2+} from its ground state. This model does not apply to $Cd_{1-x}Fe_xTe$, which manifests Van Vleck paramagnetism and has to be dealt with separately.[20]

At magnetic fields $H \ll |J_1/\mu_B|$, the ground state for a nearest-neighbor (NN) pair of ions is nonmagnetic (i.e., $\langle S_z\rangle_1^p = 0$). Therefore, the mean value of the magnetic moment for an ensemble of ions of spin S_i at a temperature T, considering only NN interactions, is given by Eq. (3) as

$$\langle S_z\rangle_1 = P_1^s(x)\langle S_z\rangle_1^s = -\frac{\overline{x}}{x} S_i \mathcal{B}_{S_i}(\eta) \tag{4}$$

where $\eta = S_i g_i \mu_B H/k_B T_{\rm eff}$ and $\mathcal{B}_{S_i}(\eta)$ is the Brillouin function.[21] The *effective concentration* $\overline{x}(x,t) < x$ reflects the decreasing contribution of single ions to M_m. In addition, the much weaker, long-range, more distant-neighbor coupling of magnetic ions can be accounted for by an *effective temperature* $T_{\rm eff} = T + T_{\rm AF}$, where $T_{\rm AF}(x,T) > 0$. Hence, the magnetization of DMS's with spherically symmetric magnetic ions, assuming strong interactions only up to first neighbors, is given by

$$M_m = \frac{g_i \mu_B N_A}{W(x)} \overline{x} S_i \mathcal{B}_{S_i}\left(\frac{g_i \mu_B H}{k_B T_{\rm eff}}\right) + \chi_{\rm dia} H. \tag{5}$$

Besides the modified-Brillouin-function contribution of single ions to the magnetization, saturating at low fields, there can also be a significant high-field susceptibility contribution due to second- and more distant-neighbor pairs of magnetic ions.[22,23]

Combining the different interactions, and taking the zero of the energy scale at the valence-band maximum in zero field, the allowed magneto-optical transitions[16] have the energies

$$E(m_J^v \to m_J^c) = E_{gx} + \tfrac{1}{2}\hbar(\omega_0^c + \omega_0^v) + (m_J^c g_c^* - m_J^v g_v^*)\mu_B H + [E_c^{\rm ex}(m_J^c) - E_v^{\rm ex}(m_J^v)]. \tag{6}$$

Here the first term (E_{gx}) corresponds to the exciton band gap, inclusive of the excitonic diamagnetic shift, the second to Landau shifts, the third corresponds to the intrinsic Zeeman splittings of the bands, and the fourth is due to the sp-d exchange. These transitions obey the selection rule

$$\Delta m_J = m_J^c - m_J^v = 0, \pm 1. \tag{7}$$

At low temperatures, the single excitonic transition in the absence of a magnetic field splits into four components for $H > 0$ in the Faraday geometry (i.e., for light propagation along **H**), with $\Delta m_J = \pm 1$ and energies given by

$$E_a(-\tfrac{3}{2} \to -\tfrac{1}{2}) = E_{gx} + \tfrac{1}{2}\hbar(\omega_0^c + \omega_0^v) - \tfrac{1}{2}(g_c^* - 3g_v^*)\mu_B H - \tfrac{1}{2}N_0(\alpha - \beta)x\langle\langle S_z\rangle\rangle, \tag{8}$$

$$E_b(-\tfrac{1}{2} \to \tfrac{1}{2}) = E_{gx} + \tfrac{1}{2}\hbar(\omega_0^c + \omega_0^v) + \tfrac{1}{2}(g_c^* + g_v^*)\mu_B H + \tfrac{1}{2}N_0(\alpha + \beta/3)x\langle\langle S_z\rangle\rangle, \tag{9}$$

$$E_c(\tfrac{1}{2} \to -\tfrac{1}{2}) = E_{gx} + \tfrac{1}{2}\hbar(\omega_0^c + \omega_0^v) - \tfrac{1}{2}(g_c^* + g_v^*)\mu_B H - \tfrac{1}{2}N_0(\alpha + \beta/3)x\langle\langle S_z\rangle\rangle, \tag{10}$$

$$E_d(\tfrac{3}{2} \to \tfrac{1}{2}) = E_{gx} + \tfrac{1}{2}\hbar(\omega_0^c + \omega_0^v) + \tfrac{1}{2}(g_c^* - 3g_v^*)\mu_B H + \tfrac{1}{2}N_0(\alpha - \beta)x\langle\langle S_z\rangle\rangle, \tag{11}$$

These components, shown schematically in Fig. 1, are circularly polarized, the a and b transitions allowed for $\hat{\boldsymbol{\sigma}}_+ = (1/\sqrt{2})(\hat{\mathbf{x}} + i\hat{\mathbf{y}})$ whereas c and d transitions occur for $\hat{\boldsymbol{\sigma}}_- = (1/\sqrt{2})(\hat{\mathbf{x}} - i\hat{\mathbf{y}})$. In the Voigt geometry (i.e., for light propagation normal to **H**), the a, b, c, and d components are polarized normal to **H**; in addition, two transitions, governed by $\Delta m_J = 0$ and polarized along **H**, are expected at

$$E_e(-\tfrac{1}{2} \to -\tfrac{1}{2}) = E_{gx} + \tfrac{1}{2}\hbar(\omega_0^c + \omega_0^v) - \tfrac{1}{2}(g_c^* - g_v^*)\mu_B H - \tfrac{1}{2}N_0(\alpha - \beta/3)x\langle\langle S_z\rangle\rangle, \tag{12}$$

$$E_f(\tfrac{1}{2} \to \tfrac{1}{2}) = E_{gx} + \tfrac{1}{2}\hbar(\omega_0^c + \omega_0^v) + \tfrac{1}{2}(g_c^* - g_v^*)\mu_B H + \tfrac{1}{2}N_0(\alpha - \beta/3)x\langle\langle S_z\rangle\rangle, \tag{13}$$

IV. RESULTS AND DISCUSSION

A. $Cd_{1-x}Mn_xTe$

The electronic configuration of free Mn^{2+} is $[Ar]3d^5$ and, following Hund's rules, its ground state is $^6S_{5/2}$. As a substitutional ion replacing Cd^{2+} and hence with T_d site symmetry in CdTe, the sixfold spin degeneracy of $^6S_{5/2}$ is lifted by the crystal-field effects, yielding a Γ_8 quadruplet ground state and a Γ_7 doublet 0.001 meV above it.[24] This splitting being so small, it is justified to treat the ground state of Mn^{2+} as an atomic $^6S_{5/2}$ level. Since the first crystal-field-split excited state $[^4G(^4\Gamma_4)]$ is $\sim$2.2 eV above the ground state,[25] at low temperatures only the $^6S_{5/2}$ state is populated and Mn^{2+} ions in CdTe exhibit paramagnetism with an effective spin $S_i = \frac{5}{2}$.

The sample used in this investigation has a nominal Mn concentration of $x = 0.01$. Microprobe analysis of the sample yielded $x = 0.0097 \pm 0.0005$, in good agreement with the nominal value. The zero-field position of the free exciton at

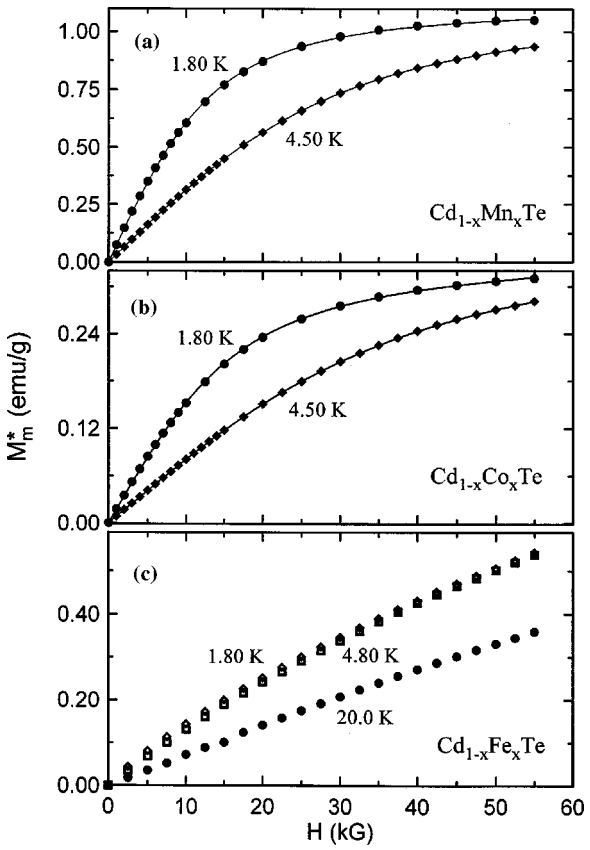

FIG. 2. Magnetization (corrected for the host diamagnetism) as a function of field: (a) $Cd_{1-x}Mn_xTe$ specimen at 1.80 and 4.50 K; (b) $Cd_{1-x}Co_xTe$ specimen at 1.80 and 4.50 K; and (c) $Cd_{1-x}Fe_xTe$ specimen at 1.80, 4.80, and 20.0 K.

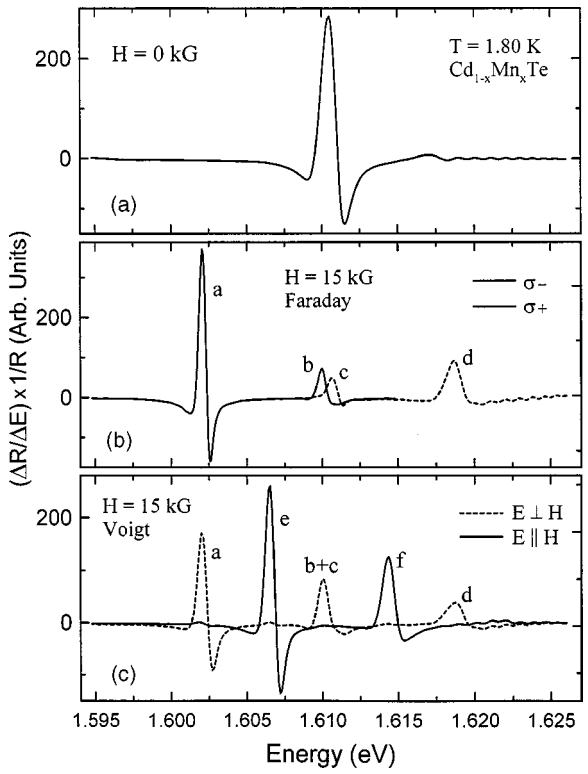

FIG. 3. Excitonic signatures of $Cd_{1-x}Mn_xTe$ at 1.80 K: (a) $H=0$; and $H=15$ kG in the (b) Faraday and (c) Voigt geometry.

1.80 K is $1.611\,35\pm0.000\,05$ eV, corresponding to a shift of 14.75 ± 0.05 meV from that of CdTe; this shift also yields $x\sim0.01$.[25]

The magnetization of the $Cd_{1-x}Mn_xTe$ specimen as a function of the magnetic field (corrected for the host diamagnetism) at 1.80 and at 4.50 K is shown in Fig. 2(a). The solid lines are Brillouin-function fits to the data points based on Eq. (5). As can be seen, for both temperatures the magnetization is linear in H at low fields, but approaches saturation at high fields. From a least-squares fit of the data to Eq. (5), using the values of $g_{Mn^{2+}}=2.00$ and $S_{Mn^{2+}}=\frac{5}{2}$, the fitting parameters $\overline{x}$ and T_{AF} obtained for each temperature are, at 1.80 K, $\overline{x}=0.0090$ and $T_{AF}=0.47$ K, and, at 4.50 K, $\overline{x}=0.0092$ and $T_{AF}=0.64$ K. Using $|J_1/k_B|\simeq6$ K for $Cd_{1-x}Mn_xTe$,[26] and considerations based on the nearest-neighbor probability distribution, the actual concentration of magnetic ions x can be extracted from $\overline{x}$. The x's thus deduced, 0.0101 for 1.80 K and 0.0103 for 4.50 K, are in excellent agreement with both the nominal and the microprobe values and indicate that the exchange interaction among the Mn^{2+} ions does not extend beyond the first neighbors. Finally, a fitting of the high-temperature susceptibility ($100<T<300$ K) for this sample in the linear regime[27] results in $x=0.0100\pm0.0003$.

An illustrative example of the excitonic Zeeman effect in $Cd_{1-x}Mn_xTe$ is displayed in Fig. 3. The strong zero-field $1s$ free-exciton signature at 1.80 K is shown in Fig. 3(a). It appears at $E_{gx}=1.611\,35\pm0.0005$ eV and is very sharp, with a broadening of less than 1 meV. This broadening value is remarkably small for the linewidth of an exciton in a ternary alloy, and is a testimony to the high quality of the crystal. Figures 3(b) and 3(c) show the Zeeman components of the $1s$ free exciton observed in the Faraday and Voigt geometries, respectively, at 15 kG. In agreement with Fig. 1, the free exciton splits into four lines (labeled *a*, *b*, *c*, and *d*) in the Faraday geometry, *a* and *b* in the $\hat{\boldsymbol{\sigma}}_+$ and *c* and *d* in the $\hat{\boldsymbol{\sigma}}_-$ circular polarizations. In the Voigt geometry, two additional lines, *e* and *f*, appear linearly polarized parallel to **H**, while *a*, *b*, *c*, and *d* are polarized normal to **H**.

The excitonic Zeeman splitting of the free exciton vs magnetic field for the $Cd_{1-x}Mn_xTe$ sample at 1.80 K is shown in Fig. 4. All the six branches saturate to some constant value for fields above ~30 kG, and they are approximately linear in field below ~10 kG. Besides these, three additional branches appear in the spectra for fields above ~20 kG, labeled as 1, 2, and 3 in Fig. 4. Although branch 2 follows the same Brillouin-function behavior as do the six Zeeman components, 1 and 3 display a linear field dependence, showing no sign of saturation even at the highest fields. Twardowski, Nawrocki, and Ginter[28] have also reported these branches; they attribute the features that saturate at higher fields to the $2s$ and $3s$ excited states of the free exciton, and those with a linear field dependence to higher-lying Landau levels. The fact that all of these features have energies above the $1s$ exciton energy is consistent with these conclusions.

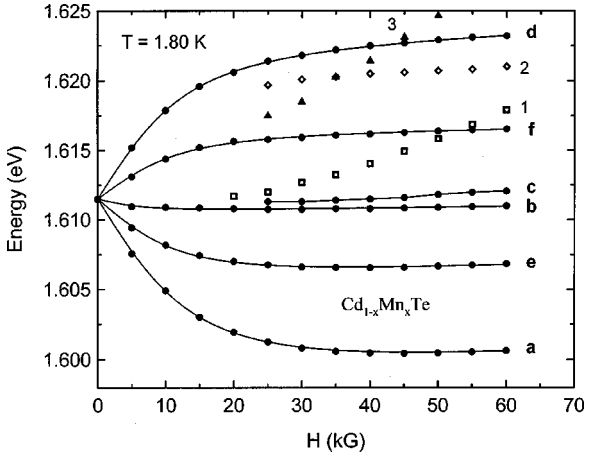

FIG. 4. Zeeman components of the free exciton for $Cd_{1-x}Mn_xTe$ at 1.80 K as a function of magnetic field.

The spacings between the Zeeman components *a*, *e*, and *f* (Fig. 4) vs the corresponding magnetization at 1.80 K [Fig. 2(a)] are displayed in Fig. 5. These three lines were selected because they are the strongest and sharpest of the six Zeeman components for most of the magnetic-field range covered, and/or because their positions could be determined without any ambiguity, since they are free from the proximity of other features. Using the expressions obtained for the positions of these lines in Eqs. (8)–(13), the corresponding splittings are given by

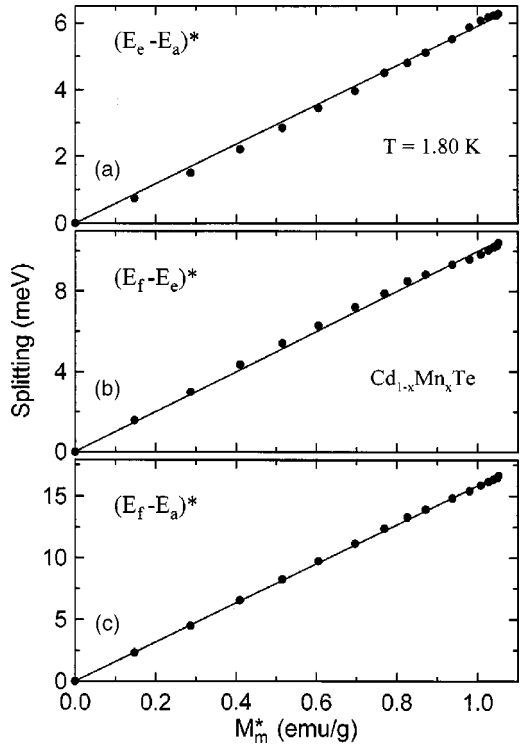

FIG. 5. Excitonic Zeeman splitting as a function of magnetization at 1.80 K: (a) E_e-E_a; (b) E_f-E_e; and (c) E_f-E_a. The spectroscopic data are corrected due to the intrinsic Zeeman shifts of the carriers and the magnetization for the diamagnetism of the host. The linear least-squares fits to the data are also shown.

$$E_e-E_a=-g_v^*\mu_B H+\tfrac{1}{3}N_0\beta_x\langle\langle S_z\rangle\rangle, \tag{14}$$

$$E_f-E_e=(g_c^*-g_v^*)\mu_B H-\tfrac{1}{3}N_0(3\alpha-\beta)x\langle\langle S_z\rangle\rangle. \tag{15}$$

Note that the first term in each of the above equations, related to the intrinsic spin splitting of the bands, is a linear function of the field, while the second term is related to the magnetization through Eq. (11). Therefore, the splittings, corrected for the intrinsic spin contributions, can be expressed as a function of magnetization (already corrected for the host diamagnetism) as

$$(E_e-E_a)^*=-C_0N_0\beta M_m^*, \tag{16}$$

$$(E_f-E_e)^*=C_0N_0(3\alpha-\beta)M_m^*, \tag{17}$$

where $C_0=W(x)/3N_A\mu_B g_i$. Based on these equations, the corrected Zeeman splittings are clearly seen to be linear functions of M_m^*, and their slopes yield $N_0\alpha$ and $N_0\beta$.

For the $Cd_{1-x}Mn_xTe$ sample used ($x=0.01$), $W(x)=239.4$ g/mole. With $g_{Mn^{2+}}=2.00$, $g_c^*=-1.59$,[29] $g_v^*=-0.04$,[30,31] and the slopes from the linear least-squares fits to the data in Fig. 5, one obtains $N_0\alpha=191\pm5$ meV and $N_0\beta=-826\pm14$ meV.

B. $Cd_{1-x}Co_xTe$

The energy-level spectrum and magnetic properties of free Co^{2+} in DMS's having T_d site symmetry have been studied by Villeret, Rodriguez, and Kartheuser.[13] The electronic configuration of Co^{2+} is $[Ar]3d^7$ and hence it has a $^4F_{9/2}$ ground state. Under the influence of the crystal field of a T_d site in CdTe, its sevenfold orbital degeneracy splits into a $^4\Gamma_2$ singlet, a $^4\Gamma_5$ triplet, and a $^4\Gamma_4$ triplet in the order of increasing energy. The crystal-field-splitting energy between the ground state $^4\Gamma_2$ and the first excited state $^4\Gamma_5$ is $\Delta=390.5$ meV.[32] Therefore, only the ground state is populated at low temperatures. Spin-orbit coupling then splits each of the $^4\Gamma_5$ and $^4\Gamma_4$ into $\Gamma_6+\Gamma_7+2\Gamma_8$ levels, as shown in Fig. 6.[33] The ground state $^4\Gamma_2$ does not split but becomes Γ_8, retaining its fourfold spin degeneracy. Thus, at 1.80 K, the Co^{2+} ion behaves paramagnetically with an effective spin $S_i=\frac{3}{2}$.

The results reported in this section are based on a $Cd_{1-x}Co_xTe$ specimen having a nominal value of $x=0.01$. Microprobe analysis of the sample yielded $x=0.0065\pm0.0010$. The magnetization of the sample at 1.80 and at 4.50 K as a function of the magnetic field (corrected for the host diamagnetism) is shown in Fig. 2(b). The solid lines are Brillouin-function fits to the data points based on Eq. (5). As can be seen, at both temperatures, the magnetization is linear in H at low fields, but approaches saturation at the higher fields. It should be noted that, despite the low Co concentration, the saturation in the magnetization curve is very similar to that of the $Cd_{1-x}Mn_xTe$ sample with a *higher* Mn concentration [Fig. 2(a)]. This is an indication of a stronger AF interaction among Co^{2+} ions compared to Mn^{2+} ions. From a least-squares fit of the data to Eq. (5), using the values of $g_{Co^{2+}}=2.3093$,[34] and $S_{Co^{2+}}=3/2$,[35] the fitting parameters $\overline{x}$ and T_{AF} were obtained for each temperature. It was found

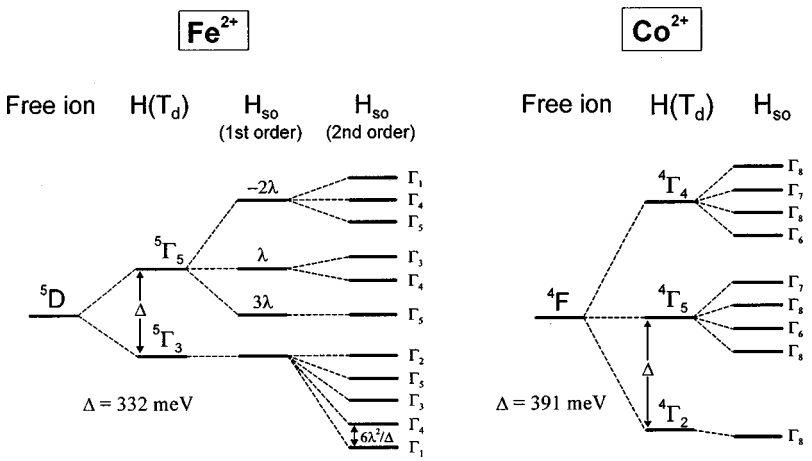

FIG. 6. Schematic diagram of the energy levels of Co^{2+} and Fe^{2+} ions in a T_d field, taking into account the spin-orbit interaction [following Rodriguez *et al.* (Ref. 43)].

that $\overline{x}=0.0035$ and $T_{AF}=0.39\,K$ at 1.80 K, whereas $\overline{x}=0.0038$ and $T_{AF}=0.47\,K$ at 4.50 K. A fitting of the high-temperature susceptibility ($100<T<300\,K$) for this sample in the linear regime yielded $x=0.0053\pm0.0002$. Note that these results indicate that $\overline{x}/x=0.66\pm0.07$, a value much smaller than the 0.95 obtained from the NN probability distribution.[18,19] Thus it appears that, in contrast to the case of Mn^{2+} in CdTe, the AF interactions are not limited to NN Co^{2+} ions, but extend to more distant neighbors as well. This is in agreement with the large value of $|J|$ for $Cd_{1-x}Co_xTe$, about five times larger than that for $Cd_{1-x}Mn_xTe$, as observed in a fit to high-temperature susceptibility of this and other samples.[36]

An illustrative example of the excitonic Zeeman effect in $Cd_{1-x}Co_xTe$ is displayed in Fig. 7. The strong zero-field $1s$ free-exciton signature at 1.80 K [Fig. 7(a)] appears at $E_{gx}=1.606\,64\pm0.000\,05\,eV$ with a broadening of less than 2 meV. Figures 7(b) and 7(c) show the splitting of the $1s$ free exciton for a field of 60 kG in the Faraday and Voigt geometries, respectively. A comparison with the results in $Cd_{1-x}Mn_xTe$ (Fig. 3) reveals an intriguing difference: in $Cd_{1-x}Co_xTe$, the inner Zeeman components appear in the sequence *b*, *e*, *f*, and *c* with increasing energy, in contrast to the sequence *e*, *b*, *c*, and *f* in $Cd_{1-x}Mn_xTe$. This sequence has an important consequence for the value of $N_0\alpha$ in $Cd_{1-x}Co_xTe$.

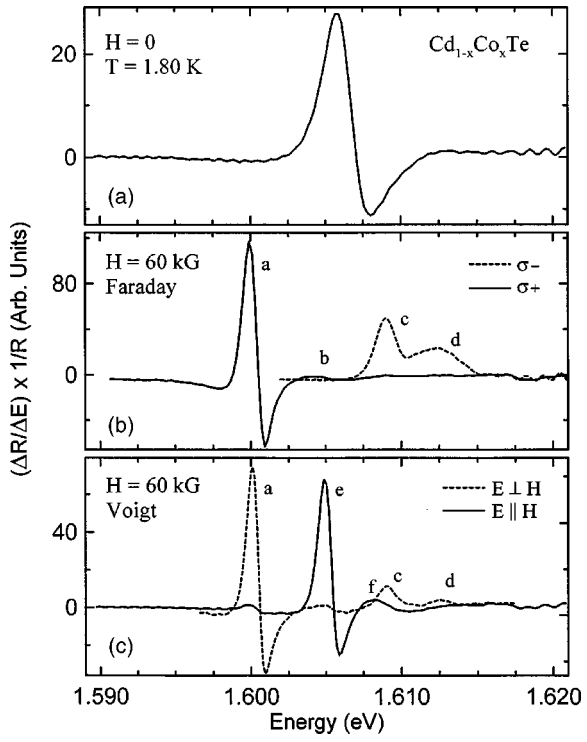

FIG. 7. Excitonic signatures of the $Cd_{1-x}Co_xTe$ specimen at 1.80 K: (a) $H=0$; and $H=60\,kG$ in the (b) Faraday (c) Voigt geometry.

The Zeeman splitting of the free exciton as a function of magnetic field for the $Cd_{1-x}Co_xTe$ sample at 1.80 K is shown in Fig. 8. All the six branches saturate to some constant value for fields above 40 kG, and they are approximately linear in field for $H<10\,kG$. The excitonic diamagnetic shift[31,37] can also be clearly seen here as an upward shift of the Zeeman components at high fields. Comparing this figure with Fig. 4 for $Cd_{1-x}Mn_xTe$, two major differences can be observed. First, the sequence in which the Zeeman components occur for the two are different, as was mentioned above. Second, the energy differences (E_e-E_b) and (E_c-E_f) are quite small for $Cd_{1-x}Co_xTe$, even for the highest fields; they are less than $\sim$0.7 meV at 60 kG. In order to extract the physical significance of these experimental observations, it is useful to express (E_e-E_b) and (E_c-E_f) from Eqs. (8)–(13), i.e.,

$$(E_b-E_e)=g_c^*\mu_B H+N_0\alpha x\langle\langle S_z\rangle\rangle, \tag{18}$$

$$E_c-E_f=-g_c^*\mu_B H-N_0\alpha x\langle\langle S_z\rangle\rangle. \tag{19}$$

Given $g_c^*=-1.59$,[29] at 60 kG the intrinsic contribution to the spacings is $\sim$0.6 meV, clearly indicating that the (b,e) and (f,c) splittings are essentially intrinsic in their origin. Dictated by the experimental error in the measured values of the splittings ($\sim$0.1 meV), an upper limit for $|N_0\alpha|$ is estimated at 20 meV. Finally, comparing the spacings (E_d-E_c) and (E_b-E_a) in Fig. 8, a small difference can observed; based on the Heisenberg-type interaction of Eq. (2), there should be no difference between the two. This asymmetric spin splitting is an indication of a second-order, non-

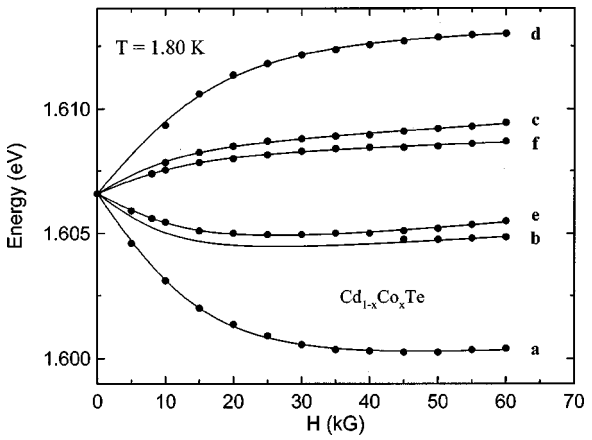

FIG. 8. Zeeman components of the free exciton for $Cd_{1-x}Co_xTe$ at 1.80 K as a function of magnetic field.

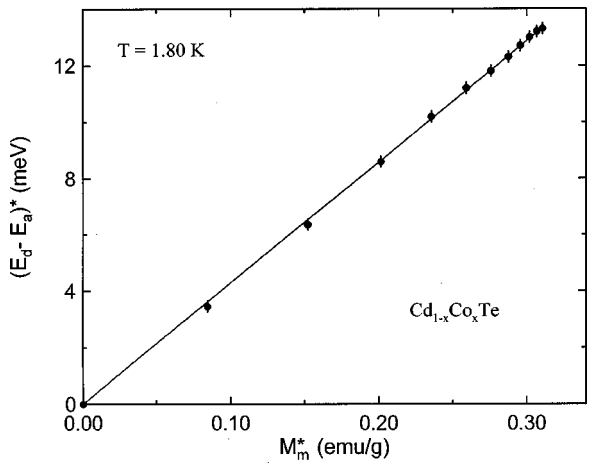

FIG. 9. Excitonic Zeeman splitting $E_d - E_a$ of $Cd_{1-x}Co_xTe$ as a function of magnetization at 1.80 K. The spectroscopic data are corrected for the intrinsic Zeeman shifts of the bands and the magnetization for the diamagnetism of the host. The linear least-squares fit to the data is also shown.

Heisenberg-type exchange interaction between the Co^{2+} spins and the effective hole spins.[38]

Combining the results in Figs. 2(b) and 8, one can display the spacing between the outer Zeeman components, $(E_d - E_a)$, as a function of magnetization at 1.80 K. These components were selected to avoid any anomaly due to the asymmetric splitting mentioned above. Using the expressions obtained for the energy positions of d and a [Eqs. (8) and (13)],

$$E_d - E_a = (g_c^* - 3g_v^*)\mu_B H + N_0(\alpha - \beta)x\langle\langle S_z\rangle\rangle. \quad (20)$$

Hence, the spacing (corrected for the intrinsic spin contributions) and magnetization (already corrected for the host diamagnetism) yield

$$(E_d - E_a)^* = C_0 N_0(\alpha - \beta)M_m^*, \quad (21)$$

where $C_0 = W(x)/N_A\mu_B g_i$. Thus, the corrected Zeeman splitting is a linear function of M_m^*, and its slope gives $N_0(\alpha - \beta)$.

For the $Cd_{1-x}Co_xTe$ specimen studied, i.e., with $x = 0.006$, $W(x) = 239.7$ g/mole; $g_{Co^{2+}} = 2.3094$,[34] $g_c^* = -1.59$, $g_v^* = -0.04$; the slope obtained from the linear least-squares fit to the data in Fig. 9 yields $N_0(\alpha - \beta) = 2331 \pm 130$ meV. Given the upper limit of 20 meV obtained above for $|N_0\alpha|$ and the error bracket of 130 meV, it is justifiable to set $N_0\beta = -2331 \pm 130$ meV.

C. $Cd_{1-x}Fe_xTe$

The energy-level scheme and magnetic properties of free Fe^{2+} in DMS's with T_d site symmetry have been studied by Villeret, Rodriguez, and Kartheuser.[13] The electronic configuration of Fe^{2+} is $[Ar]3d^6$ which, following Hund's rules, has the $^5D_4$ ground state. Under the influence of the crystal field of a T_d site in CdTe, the fivefold-degenerate orbital state splits into a $^5\Gamma_3$ doublet ground state and a $^5\Gamma_5$ triplet excited state, with a crystal-field splitting of $\Delta = 332$ meV.[35] Thus only the ground state is appreciably populated at low temperatures. The spin-orbit interaction splits the $^5\Gamma_3$ ground state, in order of increasing energy, into a singlet Γ_1, a triplet Γ_4, a doublet Γ_3, a triplet Γ_5, and a singlet Γ_2, as shown in Fig. 6. Since the Γ_1 ground state of Fe^{2+} is nonmagnetic, $Cd_{1-x}Fe_xTe$ does not exhibit ordinary paramagnetism. However, in the presence of a magnetic field, the Zeeman interaction mixes the ground state with the low-lying excited states, leading to the temperature-independent Van Vleck paramagnetism.[20]

The results reported in this section are based on a $Cd_{1-x}Fe_xTe$ specimen with a nominal Fe concentration of $x = 0.01$; microprobe analysis of the sample yielded $x = 0.007 \pm 0.001$. The zero-field position of the free exciton at 4.80 K is 1.6095 ± 0.0001 eV, corresponding to a shift of 12.9 ± 0.1 meV from that of CdTe. This shift yields $x = 0.0072$, in agreement with the microprobe result. The magnetization of the sample at 1.80, 4.80, and 20.0 K as a function of the magnetic field (corrected for the host diamagnetism) is shown in Fig. 2(c). The anisotropy of the magnetization as a function of crystallographic direction relative to the field direction can be ignored here in view of the small value of x and the relatively small magnetic fields used. As can be seen, the magnetization is almost linear at all three temperatures and does not saturate up to the highest fields, despite the small concentration of Fe. This is in striking contrast to the Brillouin-function behavior of $Cd_{1-x}Mn_xTe$ and $Cd_{1-x}Co_xTe$ shown in Figs. 2(a) and 2(b), and constitutes a strong signature of the Van Vleck paramagnetism unique to Fe- (and Cr) based DMS's. Another manifestation of Van Vleck paramagnetism is the temperature independence of magnetization at lower temperatures, also evident in Fig. 2, the magnetization at 1.80 and 4.80 K being almost identical.

The Zeeman splitting of the free exciton as a function of magnetic field for the $Cd_{1-x}Fe_xTe$ sample at 4.80 K is shown in Fig. 10. Comparing this figure with Fig. 4 for $Cd_{1-x}Mn_xTe$ and Fig. 8 for $Cd_{1-x}Co_xTe$, two major differences can be noticed immediately. First, none of the four branches saturate to some constant value, even for the highest fields. Secondly, they are approximately linear in H for

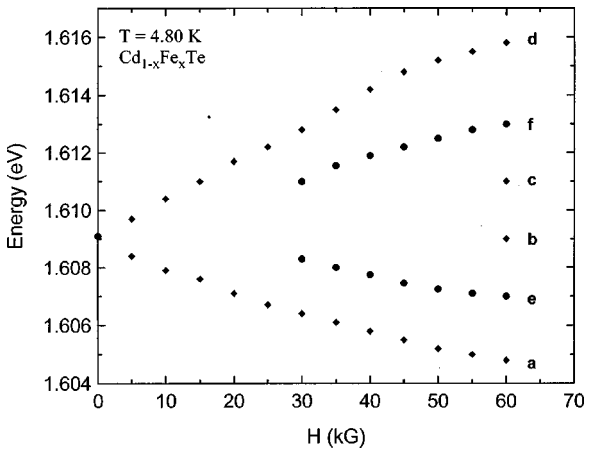

FIG. 10. Zeeman components of the free exciton for $Cd_{1-x}Fe_xTe$ at 4.80 K as a function of magnetic field.

the entire range of fields, despite the small value of x. Also, the Zeeman splittings are approximately independent of temperature below ~5 K. All of these trends are in accordance with those shown in Fig. 2 for the magnetization of this sample, being direct consequences of Van Vleck paramagnetism. Finally, the excitonic diamagnetic shift is clearly displayed by the upward shift of the Zeeman components at high fields.

Combining the spectroscopic and magnetization data, Fig. 11 displays the spacing between the outer Zeeman components, (E_d-E_a), and that between the inner components, (E_f-E_e), as a function of magnetization of the same $Cd_{1-x}Fe_xTe$ sample, all at 4.80 K. These Zeeman components were selected because the third pair of components (b and c) could not be resolved except at the highest field. Solving Eqs. (17) and (21) simultaneously using the slopes from Fig. 11, the values of $N_0\alpha$ and $N_0\beta$ can be readily obtained. For the $Cd_{1-x}Fe_xTe$ specimen used ($x=0.007$), $W(x)$

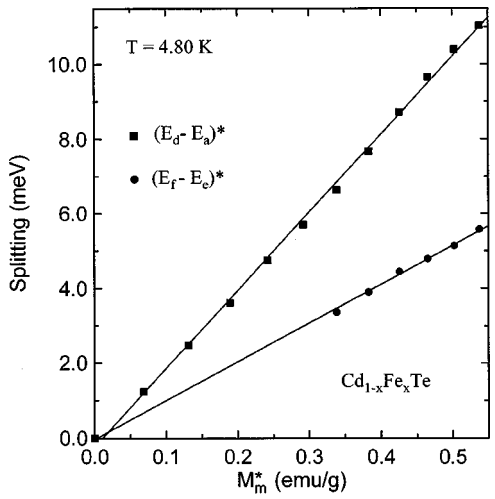

FIG. 11. Excitonic Zeeman splittings of $Cd_{1-x}Fe_xTe$ as a function of magnetization at 4.80 K. The spectroscopic data are corrected due to the intrinsic Zeeman shifts of the carriers and the magnetization for the diamagnetism of the host. The linear least-squares fits to the data are also shown.

TABLE I. The sp-d exchange constants (in meV) obtained from the present study and those reported in the literature. The technique used for each case is also given. WMR indicates wavelength-modulated reflectivity, UR unmodulated reflectivity, and UT unmodulated transmission, and SFR spin-flup Raman scattering.

$N_0\alpha$	$N_0\beta$	Technique	Reference
	$Cd_{1-x}Mn_xTe$		
191 ± 5	-826 ± 14	WMR	Present study
220 ± 10	-880 ± 40	UR	7
216 ± 25	-840 ± 25	UR	28
194		SFR	40
	$Cd_{1-x}Co_xTe$		
<20	-2331 ± 130	WMR	Present study
	$Cd_{1-x}Fe_xTe$		
311 ± 5	-842 ± 14	WMR	Present study
300 ± 40	-1270 ± 80	UT and UR	39

$=239.6$ g/mole; using the analysis in Ref. 39, $g_c^*=-1.59$, $g_v^*=-0.04$, and the slope from the linear least-squares fit to the data in Fig. 11, one obtains $N_0\alpha=269\pm17$ meV and $N_0\beta=-836\pm29$ meV.

V. CONCLUDING REMARKS

As emphasized in the Introduction and in the theoretical Sec. III, the striking magnetic phenomena displayed by the II-VI DMS's can be traced to (1) the sp-d exchange interaction between the spins of the magnetic ions and those of the band electrons, characterized by $N_0\alpha$ and $N_0\beta$, and (2) the d-d exchange interaction between the spins of the magnetic ions, expressed by $J_1, J_2, \ldots$. The observation and identification of all the six excitonic Zeeman components for Mn^{2+} and Co^{2+} have allowed both $N_0\alpha$ and $N_0\beta$ to be separately determined rather than just $N_0(\alpha-\beta)$, as in the excitonic Faraday effect.[4] In Table I we list $N_0\alpha$ and $N_0\beta$ for Mn^{2+}, Co^{2+}, and Fe^{2+} as the magnetic ions in the zinc-blende CdTe host and compare them with values reported in the literature.

(i) $Cd_{1-x}Mn_xTe$. The values of $N_0\alpha$ and $N_0\beta$ obtained in the present investigation have smaller error bars due to the sharp signatures observed in modulation spectroscopy, the exceptional optical quality of the specimens employed, and the use of calibration lines to determine the energies of the Zeeman components more precisely. It is gratifying to note that the value of 175 meV quoted for $N_0\alpha$ by Peterson *et al.*[40] from their spin-flip Raman scattering for a sample with $x=0.01$ yields 194 meV when corrected for $\overline{x}/x=0.9$, as in the present measurement. The values reported by Gaj, Planel, and Fishman[7] and by Twardowski, Nawrocki, and Ginter[28] are somewhat higher; the difference can be attributed to two factors. First, the corrections due to the intrinsic Zeeman effect of the bands and the diamagnetism of the host should be considered when dealing with small Mn concentrations, as has been done in the present study. Second, although the experimental results in Fig. 5 show a linear relation between the Zeeman splittings and magnetization, a small departure can be observed in Figs. 5(a) and 5(b). These

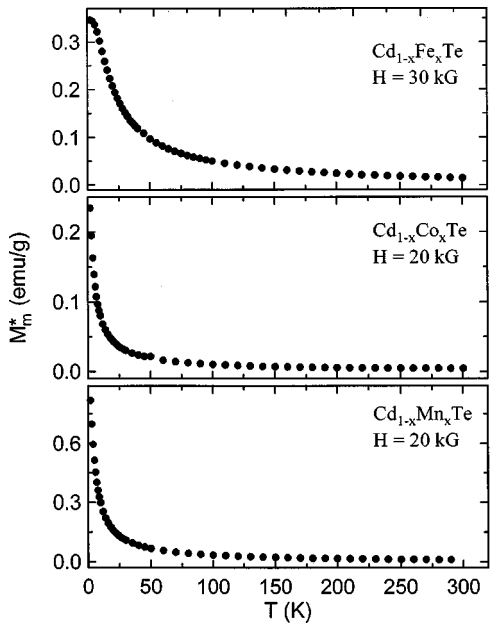

FIG. 12. Magnetization (corrected for host diamagnetism) of $Cd_{1-x}Fe_xTe$, $Cd_{1-x}Co_xTe$, and $Cd_{1-x}Mn_xTe$ as a function of temperature.

nonlinearities, whether due to higher-order terms in the exchange interaction or an experimental artifact, deserve further theoretical investigation and experimental verification.

(ii) $Cd_{1-x}Co_xTe$. The values of $N_0\alpha$ and $N_0\beta$ have been obtained independently in the present study, thanks to the observation of all six Zeeman components and the relatively larger x characterizing the sample employed compared to those employed in previous studies.[31,41] The significantly larger $|N_0\beta|$ for Co^{2+} compared to that for Mn^{2+} in CdTe is a behavior similar to that in CdSe, CdS, ZnSe, and ZnTe.[23,42] The value $|N_0\alpha|$, on the other hand, is found to have an upper limit of 20 meV based on the measurements reported here, in contrast to other II-VI DMS's studied so far, the typical value being 200–300 meV.[42] It is striking to see such a big difference in the value of α for different TMI's in a given host as well as for the same TMI in different hosts.

Based on the magnetization results, it is found that the AF d-d interaction among Co^{2+} ions is much stronger than among Mn^{2+} ions in CdTe. While this interaction is limited to NN Mn^{2+} clusters, it extends to more distant-neighbor Co^{2+} clusters. As was mentioned earlier, this is in agreement with the large values of d-d exchange constants $|J_1|$ and $|J_2|$ for Co- compared to Mn-based II-VI DMS's.[26] The large d-d interaction in $Cd_{1-x}Co_xTe$ is also consistent with the large p-d interaction reflected in the value of $N_0\beta$. According to the superexchange model of Larson *et al.*[43] developed for Mn-based DMS's, one can state roughly that a larger magnitude of β leads to a larger d-d interaction between the magnetic moments of TMI's. The large increase of $|J_1|$ and $|J_2|$ from Mn- to Co-based II-VI DMS's is indeed in accordance with the corresponding increase of $|\beta|$.

(iii) $Cd_{1-x}Fe_xTe$. Both the magnetization and the excitonic Zeeman splittings of $Cd_{1-x}Fe_xTe$ show features characteristic of Van Vleck paramagnetism at low temperatures. Temperature independence and the absence of saturation at the highest fields are two characteristics of this field-induced paramagnetism, clearly displayed in the experimental results reported in the present study. To emphasize the difference between the Van Vleck paramagnetism of Fe^{2+} and the Brillouin-function behavior of Mn^{2+} and Co^{2+}, the magnetization results for $Cd_{1-x}Fe_xTe$ as a function of temperature, along with those for $Cd_{1-x}Co_xTe$ and $Cd_{1-x}Mn_xTe$, are displayed in Fig. 12. Note the difference between the three cases in the low-temperature range below ~5 K; a smaller step size over this small range and samples with higher x can be used to show the contrast even more clearly.

Another unique characteristic of Fe-based DMS's is the anisotropy of their magnetization—and hence of the excitonic Zeeman splittings—expected as a function of crystallographic direction. This feature, fully explored by Rodriguez, Villeret, and Kartheuser,[44] is mainly due to the small energy separation of the two adjacent spin-orbit-split states of the $^5\Gamma_3$ multiplet, ~3 meV in $Cd_{1-x}Fe_xTe$. At sufficiently high magnetic fields, Zeeman splittings of the states become comparable to this spacing and, combined with the Van Vleck paramagnetic behavior of the ground state, give rise to the anisotropy in magnetization. Testelin *et al.*[45] have indeed reported such an anisotropy in the magnetization of $Cd_{1-x}Fe_xTe$ ($x=0.033$) for fields exceeding 100 kG. With the maximum field of 55 kG available to us in magnetization measurements, such an anisotropy escaped detection.

Although the $N_0\alpha$ value obtained in the present study for $Cd_{1-x}Fe_xTe$ agrees with that reported by Testelin *et al.*[39] within experimental accuracy, the value of $N_0\beta$ is significantly different between the two. Part of the difference can be attributed to the neglect of intrinsic Zeeman effects of the bands and the diamagnetism of the host referred to earlier; these corrections are more important for samples with a lower concentration of Fe.

ACKNOWLEDGMENTS

The authors are indebted to Sergio Rodriguez and M. J. Seong for stimulating discussions. They acknowledge support from the National Science Foundation Grant Nos. DMR 98-00858 and DMR 94-00415 (Material Research Science and Engineering Center).

[1] For a general overview, see articles in *Diluted Magnetic Semiconductors*, edited by J. K. Furdyna and J. Kossut, Vol. 25 of *Semiconductors and Semimetals*, edited by R. K. Willardson and A. C. Beer (Academic, New York, 1988).

[2] J. A. Gaj, J. Ginter, and R. R. Galazka, Phys. Status Solidi B **89**, 655 (1978).

[3] J. A. Gaj, R. R. Galazka, and M. Nawrocki, Solid State Commun. **25**, 193 (1978).

[4] E. Oh, A. K. Ramdas, and J. K. Furdyna, J. Lumin. **52**, 183 (1992), and references therein.
[5] E. Oh, D. U. Bartholomew, A. K. Ramdas, J. K. Furdyna, and U. Debska, Phys. Rev. B **44**, 10 551 (1991).
[6] R. Planel, J. Gaj, and C. Benoit à la Guillaume, J. Phys. (Paris), Colloq. **41**, C5-39 (1980).
[7] J. A. Gaj, R. Planel, and G. Fishman, Solid State Commun. **29**, 435 (1979).
[8] M. Cardona, Suppl. 11 of *Solid State Physics*, edited by F. Seitz and D. Turnbull (Academic, New York, 1969), p. 89.
[9] R. L. Aggarwal, Vol. 9 of *Semiconductors and Semimetals*, edited by R. K. Willardson and A. C. Beer (Academic, New York, 1972), p. 151.
[10] A. K. Ramdas, H. Alawadhi, C. Parks, Eunsoon Oh, I. Miotkowski, and S. Rodriguez, in *12th International Conference on High Magnetic Fields in the Physics of Semiconductors II*, edited by G. Landwehr and W. Ossau (World Scientific, Singapore, 1997), pp. 837–846. See Fig. I in this reference where a piezomodulated reflectivity spectrum is compared to that obtained without modulation.
[11] Quantum Design, 11578 Sorrento Valley Road, San Diego, CA 92121-1311.
[12] JEOL Ltd, 1-2 Musashino 3-chome, Akishima, Tokyo 196-8558, Japan.
[13] M. Villeret, S. Rodriguez, and E. Kartheuser, Phys. Rev. B **41**, 10 028 (1990); **42**, 11 375(E) (1990).
[14] W. Mac, N. The Khoi, A. Twardowski, J. A. Gaj, and M. Demianiuk, Phys. Rev. Lett. **71**, 2327 (1993).
[15] O. W. Shih, R. L. Aggarwal, Y. Shapira, S. H. Bloom, V. Bindilatti, R. Kershaw, K. Dwight, and A. Wold, Solid State Commun. **74**, 455 (1990); E. Kartheuser, S. Rodriguez, and M. Villeret, Phys. Rev. B **48**, 14 127 (1993).
[16] E. Burstein, G. S. Picus, H. A. Gebbie, and F. Blatt, Phys. Rev. **103**, 826 (1956).
[17] D. J. Chadi, R. M. White, and W. A. Harrison, Phys. Rev. Lett. **35**, 1372 (1975).
[18] M. M. Kreitman and D. L. Barnett, J. Chem. Phys. **43**, 364 (1965).
[19] O. Okada, J. Phys. Soc. Jpn. **48**, 391 (1980).
[20] See C. Kittel, *Introduction to Solid State Physics*, 6th ed. (Wiley, New York, 1986), p. 410 for a clear and succinct discussion of Van Vleck paramagnetism.
[21] F. Reif, *Fundamentals of Statistical and Thermal Physics* (McGraw-Hill, New York, 1965), p. 257.
[22] S. Nagata, R. R. Galazka, D. P. Mullen, H. Akbarzadeh, G. D. Khattak, J. K. Furdyna, and P. H. Keesom, Phys. Rev. B **22**, 3331 (1980).
[23] M. Zielinski, C. Rigaux, A. Lemaitre, A. Mycielski, and J. Deportes, Phys. Rev. B **53**, 674 (1996).
[24] J. Lambe and C. Kikuchi, Phys. Rev. **119**, 1256 (1960).
[25] Y. R. Lee, A. K. Ramdas, and R. L. Aggarwal, Phys. Rev. B **38**, 10 600 (1988).
[26] A number of techniques can be used to determine the d-d exchange constants J_1 and J_2. See, for example, D. U. Bartholomew, E.-K. Suh, S. Rodriguez, A. K. Ramdas, and R. L. Aggarwal, Solid State Commun. **62**, 235 (1987) (Raman scattering); B. E. Larson, K. C. Hass, and R. L. Aggarwal, Phys. Rev. B **33**, 1789 (1986) (steps in high-field magnetization); T. M. Giebultowicz, J. J. Rhyne, W. Y. Ching, D. L. Huber, J. K. Furdyna, B. Lebech, and R. R. Galazka, *ibid.* **39**, 6857 (1984) (inelastic neutron scattering); A. Lewicki, A. I. Schindler, J. K. Furdyna, and W. Giriat, *ibid.* **40**, 2379 (1989) (high-temperature magnetic susceptibility). For a comparison and summary of values obtained for different II-VI DMS's, see W. J. M. de Jonge, and H. J. M. Swagten, J. Magn. Magn. Mater. **100**, 322 (1991).
[27] J. Spalek, A. Lewicki, Z. Tarnawski, J. K. Furdyna, R. R. Galazka, and Z. Obuszko, Phys. Rev. B **33**, 3407 (1986).
[28] A. Twardowski, M. Nawrocki, and J. Ginter, Phys. Status Solidi B **96**, 497 (1979).
[29] A. Nakamura, D. Paget, C. Hermann, C. Weisbuch, and G. Lampel, Solid State Commun. **30**, 411 (1979).
[30] R. L. Aggarwal, S. N. Jasperson, P. Becla, and R. R. Galazka, Phys. Rev. B **32**, 5132 (1985).
[31] O. W. Shih, R. L. Aggarwal, T. Q. Vu, and P. Becla, Solid State Commun. **81**, 245 (1992).
[32] J. M. Baranowski, J. W. Allen, and G. L. Pearson, Phys. Rev. **160**, 627 (1967).
[33] S. Rodriguez, E. Kartheuser, and M. Villeret, in *12th International Conference on High Magnetic Fields in the Physics of Semiconductors II* (Ref. 10), pp. 825–835.
[34] F. S. Ham, G. W. Ludwig, G. D. Watkins, and H. H. Woodbury, Phys. Rev. Lett. **5**, 468 (1960).
[35] J. P. Mahoney, C. C. Lin, W. H. Brumage, and F. Dorman, J. Chem. Phys. **53**, 4286 (1970).
[36] I. Miotkowski, H. Alawadhi, M. J. Seong, A. Lewicki, V. Souw, M. McElfresh, A. K. Ramdas, S. Miotkowska, and E. Dynowska, Semicond. Sci. Technol. **16**, 118 (2001).
[37] M. Inoue, N. Adachi, I. Mogi, G. Kido, Y. Nakagawa, and Y. Oka, Physica B **184**, 441 (1993).
[38] V. G. Abramishvily, A. V. Komarov, S. M. Ryabchenko, A. I. Savchuk, and Yu. G. Semenov, Solid State Commun. **101**, 397 (1997).
[39] C. Testelin, C. Rigaux, A. Mycielski, M. Menant, and M. Guillot, Solid State Commun. **78**, 659 (1991).
[40] D. L. Peterson, A. Petrou, M. Dutta, A. K. Ramdas, and S. Rodriguez, Solid State Commun. **43**, 667 (1982).
[41] D. Coquillat, Yu. G. Rubo, A. El Quazzani, A. Ribayrol, J. P. Lascaray, and R. Triboulet, Mater. Sci. Forum **182-184**, 503 (1995).
[42] D. Heiman, in *12th International Conference on High Magnetic Fields in the Physics of Semiconductors II* (Ref. 10), pp. 847–856.
[43] B. E. Larson, K. C. Hass, H. Ehrenreich, and A. E. Carlsson, Phys. Rev. B **37**, 4137 (1988); B. E. Larson and H. Ehrenreich, *ibid.* **39**, 1747 (1989).
[44] S. Rodriguez, M. Villeret, and E. Kartheuser, Phys. Scr. T**39**, 131 (1991).
[45] C. Testelin, C. Rigaux, A. Mauger, A. Mycielski, and M. Guillot, Phys. Rev. B **46**, 2193 (1992).